



Understanding dynamics of *Plasmodium falciparum* gametocytes production: Insights from an age-structured model

Ramsès Djidjou-Demasse, Arnaud Ducrot, Nicole Mideo, Gaëtan Texier

► To cite this version:

Ramsès Djidjou-Demasse, Arnaud Ducrot, Nicole Mideo, Gaëtan Texier. Understanding dynamics of *Plasmodium falciparum* gametocytes production: Insights from an age-structured model. 2020. hal-03030234v1

HAL Id: hal-03030234

<https://hal.science/hal-03030234v1>

Preprint submitted on 11 Dec 2020 (v1), last revised 17 Feb 2022 (v3)

HAL is a multi-disciplinary open access archive for the deposit and dissemination of scientific research documents, whether they are published or not. The documents may come from teaching and research institutions in France or abroad, or from public or private research centers.

L'archive ouverte pluridisciplinaire **HAL**, est destinée au dépôt et à la diffusion de documents scientifiques de niveau recherche, publiés ou non, émanant des établissements d'enseignement et de recherche français ou étrangers, des laboratoires publics ou privés.

Understanding dynamics of *Plasmodium falciparum* gametocytes production: Insights from an age-structured model

Ramsès Djidjou-Demasse^{a,*}, Arnaud Ducrot^b, Nicole Mideo^c, Gaëtan Texier^{d,e}

^aMIVEGEC, Univ. Montpellier, IRD, CNRS, Montpellier, France

^b Normandie Univ., UNIHAVRE, LMAH, FR-CNRS-3335, ISCN, 76600 Le Havre, France

^c Department of Ecology & Evolutionary Biology, University of Toronto, Toronto, Canada

^d Aix Marseille Univ., IRD, AP-HM, SSA, VITROME, IHU Méditerranée Infection, Marseille, France

^e Centre d'Epidémiologie et de Santé Publique des Armées (CESPA), Marseille, France.

*Author for correspondence: ramses.djidjoudemasse@ird.fr

Abstract

Many models of within-host malaria infection dynamics have been formulated since the pioneering work of Anderson *et al.* in 1989. Biologically, the goal of these models is to understand what governs the severity of infections, the patterns of infectiousness, and the variation thereof across individual hosts. Mathematically, these models are based on dynamical systems, with standard approaches ranging from K -compartments ordinary differential equations (ODEs) to delay differential equations (DDEs), in order to capture the relatively constant duration of replication and bursting once a parasite infects a host red blood cell. Using malariatherapy data, which offers fine-scale resolution on the dynamics of infection across a number of individual hosts, we compare the fit of one of these standard approaches (K -compartments ODEs) with a partial differential equations (PDEs) model, which explicitly tracks the "age" of an infected cell. We find that the PDE model outperforms the K -compartments ODEs, particularly early on in infections, where ODEs wildly overestimate parasite densities. Further, the PDE model highlights a strong qualitative connection between the density of transmissible parasite stages (*i.e.*, gametocytes) and the density of host-damaging (and asexually-replicating) parasite stages, which is difficult to capture by the K -compartments ODEs model. This finding provides a simple tool for predicting which hosts are most infectious to mosquitoes —vectors of *Plasmodium* parasites— which is a crucial component of global efforts to control and eliminate malaria.

Key words. Within-host model, malaria, gametocytemia, parasitemia, infectiousness

1 Introduction

Malaria has always been a public health problem and, since the discovery of malaria parasites in human blood by Charles Laveran in 1880, remains so despite more than 100 years of research. Malaria continues to have a significant impact on the world with over 400,000 deaths alone each year [47]. It is a vector-borne disease caused by five plasmodial species: *Plasmodium falciparum*, *P. vivax*, *P. malariae*, *P. ovale*, and *P. knowlesi*, with *P. falciparum* being the most pathogenic species infecting humans [29].

The malaria parasite has a complex life cycle involving sexual reproduction occurring in the insect vector [1] and two stages of infection within a human (or animal host), a liver stage [20] and blood stage [5]. Human infection starts by the bite of an infected mosquito, which injects the sporozoite form of *Plasmodium* during a blood meal. The sporozoites enter the host peripheral circulation, and rapidly transit to the liver where they infect liver cells (hepatocytes) [20]. The parasite replicates within the liver cell before rupturing to release extracellular parasite forms (merozoites), into the host circulation, where they may invade red blood cells (RBCs) to initiate blood stage infection [36]. Then follows a series of cycles of replication, rupture, and re-invasion of the RBC. Some asexual parasite forms commit to an alternative developmental pathway and become sexual forms (gametocytes) [40]. Gametocytes can be taken up by mosquitoes during a blood meal where they undergo a cycle of sexual development to produce sporozoites [1], which completes the parasite life cycle.

The classical model of within-host parasite multiplication in malaria infections was formulated by Anderson *et al.* [3]. This model tracks uninfected red blood cells (RBCs), parasitized RBCs (pRBCs) and merozoites. The pioneer work of Anderson *et al.* [3], has been further developed in several directions including in particular immune response [21, 23–25, 30, 37, 38]. Those models use an exponential process to describe the rate of rupture of pRBCs and, as a consequence, then fail to capture realistic lifetimes of the pRBCs [42]. To correct this issue, some models of malaria infection included K -compartments ordinary differential equations (ODEs) representing a progression through a parasite’s developmental cycle [21, 26, 41, 48], or delay differential equations (DDEs) to capture the time pRBCs take to mature before producing new merozoites [9, 25, 28]. Other approaches are the use of partial differential equations (PDEs) to track the age-structure of the pRBC population [4, 13, 14, 29]. It is shown in [19] that DDEs perform better than the ODEs in representing the dynamics of red blood cells during malaria infection.

In this work, using gametocyte production as a proxy variable of infectiousness, we compared model outputs from a PDE stage-structured formulation to those from classical K -compartments ODEs. Using malariatherapy data of gametocyte densities over time, we found the PDE model performed best in representing the observed dynamics. Further, the PDE model highlights a strong qualitative connection between gametocyte density and parasitemia. However, we will show that this strong connection is difficult to capture by the K -compartments ODEs model.

2 Material and method

2.1 Data and methodology

Our analysis is based on data collected from malariatherapy taken in [18]. Indeed malaria inoculation was a recommended treatment for neurosyphilis between 1940 and 1963. We also refer to [10] for a review paper on malariatherapy and the knowledge gained in the understanding of malaria infection. The data we shall use consist in daily records of gametocyte density for twelve patients. Although malariatherapy has been dismissed for obvious ethical reasons, the advantages to use such data are multiple. Indeed patients are naive to malaria infection and the dynamics are not perturbed by anti-malarial treatments. Let us notice that such data have been widely used in the literature and in particular to estimate mathematical model parameters. We refer to [18] and the references therein.

The method we shall develop consists in devising a mathematical model to describe the intra-host development of the infection and fitting the model to the available data. The output of the mathematical model will allow us to access various quantities related to the time course of the infection, including parasitemia.

2.2 Mathematical model

As discussed above, we now present the mathematical model we shall use to recover parasitemia for twelve patients from observed time courses of gametocyte density. We shall describe the within-host malaria infection coupled with red blood cells (RBCs) production as well as immune effectors. Fig. 1 presents the flow diagram of the model considered in this note. Our model is divided into four parts: (i) uninfected RBC (uRBCs) dynamics; (ii) changes in parasite stage or parasite maturity; (iii) Gametocyte production and dynamics and (iv) immune response dynamics.

For uRBCs dynamics, we divide cells into three age classes: reticulocyte (young), mature and senescent. All three ages are vulnerable to *P. falciparum* infection. This can be different for other species of *Plasmodium*. Although we focus in this work on the case of *P. falciparum*, the model described below could be applied to study other species such as *P. vivax* or *P. malariae*, which have specific RBC-age preferences [39]. Such age-structured dynamics for uRBC are well known in the literature, see for instance [34]. For the parasites, we consider stage-structured dynamics for their development within pRBC. Here the stage is a continuous variable representing the time since the concerned RBC is parasitized. Such a continuous stage structure will allow us to track the maturity of sequestered parasites, but also to have a refined description of the pRBC rupture and of the merozoites release phenomenon. We also emphasize that such a model easily allows for inclusion of anti-malarial treatments acting on only some parasite developmental stages.

Uninfected RBC dynamics. We denote by $R_r(t)$, $R_m(t)$ and $R_s(t)$ respectively the density of reticulocytes, mature RBCs and senescent RBCs at time t .

In the absence of malaria parasites, the evolution of circulating red blood cells is assumed to follow a discrete age maturation system of ordinary differential equations

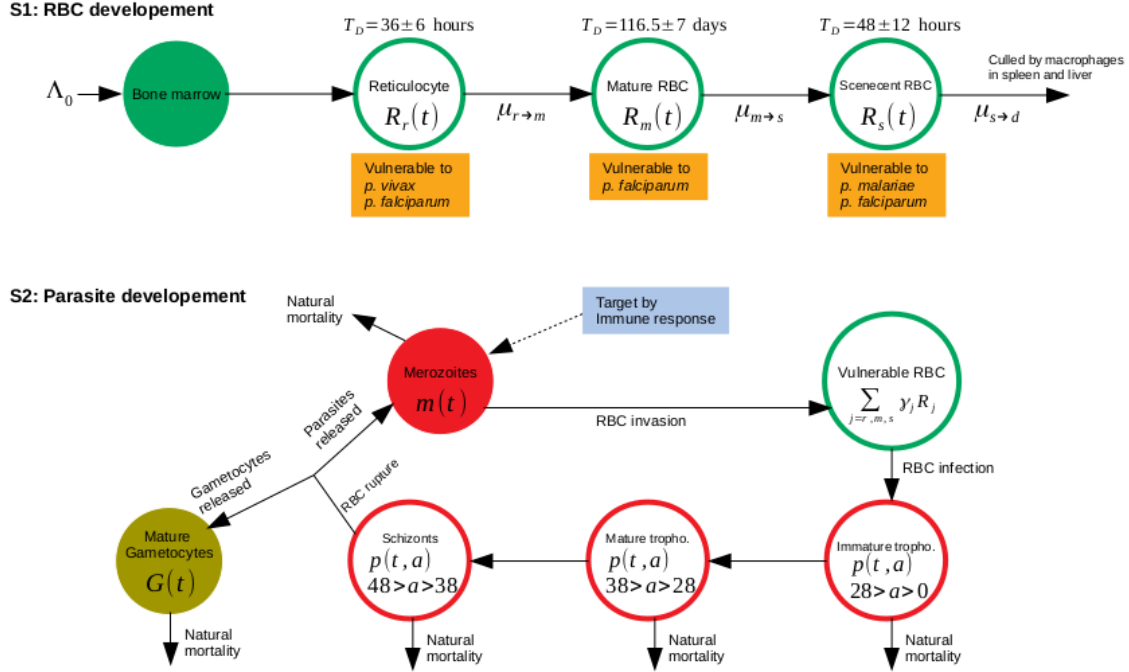


Figure 1: (S_1) The RBC development chain, (S_2) the parasite development chain. T_D = average duration (\pm one standard deviation) spent in an RBC age class given in [35], Λ_0 is the RBC production rate from the marrow source. In our model, the parameter $1/\mu_{r \rightarrow m}$ (resp. $1/\mu_{m \rightarrow s}$, $1/\mu_{s \rightarrow d}$) is the time spent in RBC reticulocyte (resp. mature, senescent) class. A continuous parameter a denotes the time since the concerned RBC is parasitized: ring stage ($0 < a < 26$ hours), trophozoite ($26 < a < 38$ hours) and schizont ($38 < a < 48$ hours). In the case of *P. falciparum* infection, one has ($\gamma_r = \gamma_m = \gamma_s = 1$) while for *P. vivax* one has ($\gamma_r = 1$, $\gamma_m = \gamma_s = 0$) and for *P. malariae* ($\gamma_r = \gamma_m = 0$, $\gamma_s = 1$) [39].

that take the form

$$\begin{cases} \frac{dR_r(t)}{dt} = \Lambda_0 - \mu_{r \rightarrow m} R_r(t), \\ \frac{dR_m(t)}{dt} = \mu_{r \rightarrow m} R_r(t) - \mu_{m \rightarrow s} R_m(t), \\ \frac{dR_s(t)}{dt} = \mu_{m \rightarrow s} R_m(t) - \mu_{s \rightarrow d} R_s(t). \end{cases} \quad (1)$$

The parameters $1/\mu_{r \rightarrow m}$, $1/\mu_{m \rightarrow s}$ and $1/\mu_{s \rightarrow d}$ respectively denote the duration of RBCs in the reticulocyte, mature and senescent age classes while Λ_0 represents the normal value of the RBC production from marrow source (i.e. the production rate of RBC). System (1) can also be found in [34].

The parameters of this system are selected from [24, 34] (see Table 1) so that in the absence of parasites, the equilibrium age distribution is given by

$$(R_r^*; R_m^*; R_s^*) = (62.50; 4853; 83.30) \times 10^6 \text{ cell/ml}. \quad (2)$$

This leads to the homeostatic equilibrium concentration of RBC ($R_r^* + R_m^* + R_s^*$) around 4.99×10^9 cells/ml which is in the range expected for humans.

Parasite dynamics with stage-structured formulation (PDE model). Here we consider the interaction between free merozoites together with the circulating RBCs. We respectively denote by $m(t)$, $p(t, a)$ and $G(t)$ the density of merozoites, parasitized RBC, and mature gametocytes at time t . The variable a denotes the time since the concerned RBC is parasitized (i.e. $\int_{a_1}^{a_2} p(t, a) da$ corresponds to the density of pRBC at time t which are infected since the time $a_1 < a < a_2$). The system we shall consider reads as:

$$\begin{cases} p(t, 0) = \beta m(t) \sum_{j=r, m, s} \gamma_j R_j(t), \\ \partial_t p(t, a) + \partial_a p(t, a) = -(\mu(a) + d_0) p(t, a), \\ \dot{m}(t) = (1 - \alpha_G) \int_0^\infty r \mu(a) p(t, a) da - \mu_m m(t) - \beta m(t) \sum_{j=r, m, s} \gamma_j R_j(t), \\ \dot{G}(t) = \alpha_G \int_0^\infty r \mu(a) p(t, a) da - \mu_G G(t). \end{cases} \quad (3)$$

We briefly sketch the interpretation of the parameters arising in (3). Parameters d_0 , μ_m and μ_G , respectively, denote the natural death rates for uRBC, for free merozoites and for mature gametocytes. Function $\mu(a)$ denotes the additional death rate of pRBC due to the parasites at stage a and leading to the rupture. The rupture of pRBC at stage a results in the release of an average number r of merozoites into the blood stream, so that pRBC then produce, at stage a , merozoites at rate $r\mu(a)$. Together with this description, the quantity $\int_0^\infty r\mu(a)p(t, a)da$ corresponds to the number of merozoites produced by pRBC at time t . The parameter β describes the contact rate between uRBC and free merozoites. Here the rupture function $\mu(a)$ is taken of the form

$$\mu(a) = \begin{cases} 0 & \text{if } a < 48h, \\ \bar{\mu} & \text{if } a \geq 48h. \end{cases}$$

Note that the probability $D(a) = \exp(-\int_0^a \mu(\sigma) d\sigma)$, that a pRBC remains parasitized after a hours of infection, takes the form $D(a) = 1$, for $a \leq 48h$ and $D(a) = e^{-(a-48)\bar{\mu}}$, for $a > 48h$. Therefore, after $48h$ (the average RBC sequestration period), D decreases

exponentially fast. Here, we fix $\bar{\mu} = 7$, and the value of $\bar{\mu}$ is not strictly significant as soon as the fast decay of D appears after 48h.

Parameters γ_k with $k = r, m, s$ describe the age preference of parasites' targets. Here we shall be concerned in *P. falciparum* infection that do not have any preference for RBC so that $\gamma_r = \gamma_m = \gamma_s = 1$. However when considering *P. vivax* infection one has $\gamma_r = 1$ and $\gamma_m = \gamma_s = 0$, so that target RBCs mostly consist in reticulocytes while when *P. malariae* infection is concerned then target RBCs are mostly senescent cells, that is $\gamma_r = \gamma_m = 0$ and $\gamma_s = 1$ [39]. The parameter α_G represents the proportion of merozoites from a bursting asexual schizonts that will enter the gametocyte compartment, i.e., are "committed" to the gametocyte developmental pathway.

Parasite dynamics with K -compartments ODEs formulation (ODE model).

For the ODE model formulation, we consider K stages for the pRBC before rupture and set $p = (p_1, p_2, p_3, \dots, p_K)$, such that $p_j(t)$ denotes the concentration of pRBC at time t . Then, setting $\dot{z} = \frac{dz}{dt}$ the ODE model writes

$$\begin{cases} \dot{p}_1(t) = \beta m(t) \sum_{j=r,m,s} \gamma_j R_j(t) - (\mu_1 + d_1) p_1(t), \\ \dot{p}_2(t) = \mu_1 p_1(t) - (\mu_2 + d_2) p_2(t), \\ \vdots \\ \dot{p}_K(t) = \mu_{K-1} p_{K-1}(t) - (\mu_K + d_K) p_K(t), \\ \dot{m}(t) = (1 - \alpha_G) r \mu_K p_K(t) - \mu_m m(t) - \beta m(t) \sum_{j=r,m,s} \gamma_j R_j(t), \\ \dot{G}(t) = \alpha_G r \mu_K p_K(t) - \mu_G G(t), \end{cases} \quad (4)$$

wherein $1/\mu_i$ and d_i are the duration of the i -stage and the death rate of pRBC respectively. The average RBC sequestration period for the K -compartments ODEs model is similar to the PDE model and writes $\frac{1}{\mu_1} + \dots + \frac{1}{\mu_K} = 48h$. Other parameters and state variables are the same as for the PDE model.

The immune responses. Following [15], here we consider two immune responses (IRs) controlling the growth of the parasite population: (i) an innate IR $S_I(t)$ at time t representing the effect of the pro-inflammatory cytokine cascade and (ii) an adaptive IR $S_A(t)$ at time t . The effect of the innate IR is a function of the present parasite (merozoite) density that takes the form

$$S_I(t) = \frac{m(t)}{m(t) + S_I^*}, \quad (5)$$

where S_I^* is the critical parasite density at which the current multiplication factor is reduced by 50%.

The adaptive IR is a function of the cumulative parasite density; this function is determined by two host-specific parameters and one constant: (1) S_A^* is the critical cumulative parasite density at which the current multiplication factor is reduced by 50%; (2) $\Delta_0 = 16$ days is the average delay required by adaptive IR to become effective [15], i.e., for time t before Δ_0 the cumulative density is set to zero (the adaptive IR has no effect and $S_A(t) = 0$ for $t \leq \Delta_0$) and (3) $\Delta_1 = 8$ days is the delay that determines the

last term in the cumulative density for times $t \geq \Delta_0$, i.e.,

$$S_A(t) = \begin{cases} \frac{\int_{\Delta_0}^t m(s)ds}{\int_{\Delta_0}^t m(s)ds + S_A^*}, & \Delta_0 \leq t < \Delta_0 + \Delta_1; \\ \frac{\int_{\Delta_0}^{\Delta_0+\Delta_1} m(s)ds}{\int_{\Delta_0}^{\Delta_0+\Delta_1} m(s)ds + S_A^*}, & t \geq \Delta_0 + \Delta_1. \end{cases} \quad (6)$$

Thus, including these two IR effects, the dynamics of asexual parasite concentration $m(t)$ should be replaced in Models (3) and (4) respectively by:

$$\dot{m}(t) = (1 - \alpha_G) \int_0^\infty r\mu(a)p(t, a)da - \left(\mu_m + \beta \sum_{j=r, m, s} \gamma_j R_j(t) + S_A(t) \right) m(t) - S_I(t), \quad (7)$$

and

$$\dot{m}(t) = (1 - \alpha_G) r\mu_K p_K(t) - \left(\mu_m + \beta \sum_{j=r, m, s} \gamma_j R_j(t) + S_A(t) \right) m(t) - S_I(t). \quad (8)$$

Initial conditions For both PDE and ODE models, the initial RBCs are assumed to be at their homeostatic equilibrium distribution in the absence of parasites given by (2), i.e., $R_r(0) = R_r^*$; $R_m(0) = R_m^*$; $R_s(0) = R_s^*$. Above models are also assumed to be free of pRBCs at the initial time, and the initial density of malaria parasites is such that $m(0) = m_0$, with m_0 a positive constant. Theses initial conditions are summarized in Table 2.

3 Results

3.1 Fitting the model parameters with data

The model presented above is fitted with the data for the time course of gametocytes of the patients. To fit our model, let us observe that most of the parameters are known from the literature [3, 18, 24, 34, 35]. Table 1 provides the values we shall use for the fixed parameters. Only three parameters need to be estimated from the data, these are: the proportion of asexual merozoites (α_G), the merozoite initial density (m_0), and the duration of sexual stage ($1/\mu_G$). These parameters are adjusted from the data for each patient by using a least square method. Basically, we find the values which minimize the difference between the ODE model prediction gametocyte density and observed data by using MatLab nonlinear least-squares solver *lsqcurvefit*. Those optimal parameters for the EDO model are then used to run the PDE model. The superposition of the data and gametocyte density output of the mathematical models are presented in Fig. 2, while the estimated parameter values for each patient are given in Table S1.

3.2 Comparison of ODE and PDE model outputs

We have presented two modelling frameworks to properly model the within-host infection of malaria. Within this context, we compare a classical model based on ordinary

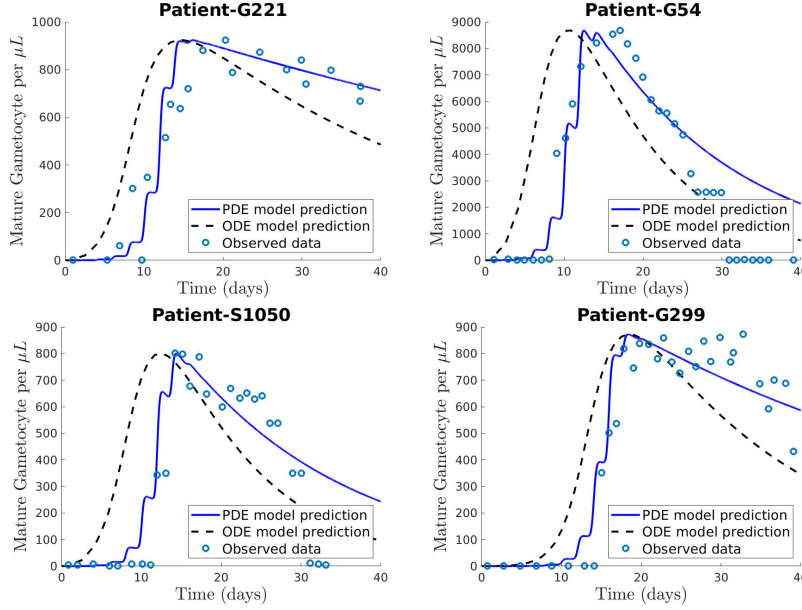


Figure 2: Comparison with data and mathematical model output for gametocyte density for patients G221, G54, S1050 and G299. Comparison for other patients is provided by Figure S1.

differential equations (ODE) with a model based on partial differential equations (PDE). Our first observation is on the parametrisation of both models. More precisely, a good description of the rupture of pRBC required at least three additional parameters and equations for the ODE model compared to PDE model; see (3) versus (4). According to the infection dynamics, our comparative results show that the PDE model fitted better the true dynamics of malaria infection, compared to the ODE model (Fig. 2). Indeed, for the initial phase of infection (approximately the first two weeks), the ODE model captures less well the delay imposed by the parasite sequestration by RBC. This sequestration period, about 48 hours for each cycle of infection by *P. falciparum*, is better highlight by the PDE model formulation (Fig. 2). Further, the goodness-of-fit of the PDE model relatively to ODE is increased when the initial parasites load m_0 is relatively high (Fig. 2, Patient-G221, G54, S1050). Next, the initial growth phase of both models seems more similar when the initial production of gametocytes is very slow and hard to find with early sampling, as a consequence of low infection densities and small fractions of pRBCs making gametocytes (Fig. 2, Patient-G299). Finally, this first wave of gametocytes development is then followed by decreasing densities for which the PDE model prediction is overall more realistic than the ODE model.

3.3 Relationship between parasitemia and gametocyte density

Our mathematical model has been fitted with the available data for each patient under consideration, which consists of gametocyte densities over time. We now use the output of this mathematical model to recover the time course of the parasitemia, defined as the

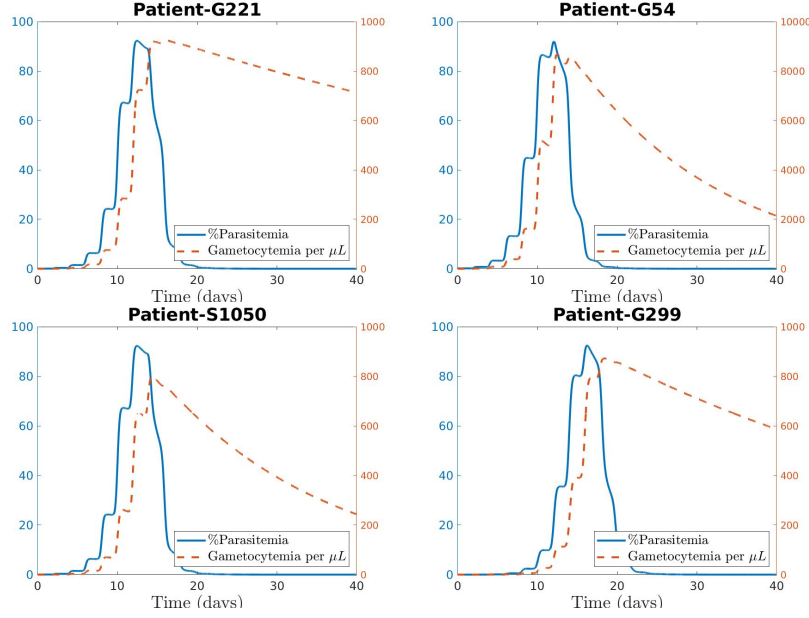


Figure 3: The time course of parasitemia and gametocyte density computed from the PDE model for patients G221, G54, S1050 and G299. Other patients are provided by Figure S2.

proportion of all infected RBC among the total number of RBC. Using the notation of the model, the parasitemia at time t , denoted by $P(t)$ can be calculated as follows

$$P(t) = \frac{\int_0^\infty p(t, a) da}{\int_0^\infty p(t, a) da + (R_r(t) + R_m(t) + R_s(t))}.$$

The time course of parasitemia, $P(t)$, computed from our model are presented in Fig. 3 for each patient together with the fitted gametocyte trajectories. As is observed for each patient, the relationship between these curves exhibits two different regimes. During some period of time $[2, T_0]$, the two curves are increasing with rather similar shape up to a time shift (of length 2 days). This means that, in this increasing regime, the gametocyte density at time t depends on the parasitemia at time $t - 2$, a delay which reflects the life cycle of the parasites inside the RBCs. After this period of increasing parasitemia and gametocyte density, namely after time T_0 , both curves are decreasing and the shapes seem to depend upon the specific patient considered. In order to make these comments more quantitative, we introduce the following formula from an estimation of the gametocyte density $G(t)$ from the parasitemia $P(t)$:

$$G(t) = \begin{cases} k_1 P(t-2)^{\theta_1} & \text{if } 2 \leq t \leq T_0 \text{ days,} \\ k_2 P(t)^{\theta_2} & \text{if } T_0 \leq t \leq 30, \end{cases} \quad (9)$$

where k_1 , k_2 , θ_1 and T_0 are four positive parameters while θ_2 is negative parameter.

In order to determine the unknown parameters k_1 , k_2 , θ_1 , θ_2 and the changing time T_0 for each patient, we perform a least square analysis. More specifically we adjust these

parameters through a logarithmic scale, that is through the following formula

$$\log_{10} G(t) = \begin{cases} \log_{10} k_1 + \theta_1 \log_{10} P(t-2) & \text{if } 2 \leq t \leq T_0, \\ \log_{10} k_2 + \theta_2 \log_{10} P(t) & \text{if } T_0 < t \leq 30. \end{cases}$$

To be more precise, our analysis couples the estimate for the time parameter T_0 , at which the above formula is changing formulation, together with two linear regressions on each part of the graph. We find that parameters k_1 , k_2 , θ_1 and T_0 are remarkably robust with respect to individuals while θ_2 depends upon each individual. The results of this analysis as well as the estimated parameters are presented in Fig. S3 and summarized by Table S2 for each patient. The quality of the fit is quantified using the coefficient of determination R^2 (for the linear regressions). It is computed for each patient and for the two regimes independently. This adjustment metric is computed using the sample of points induced by the time discretization of the partial differential equation model. For our four cases, this coefficient of determination R^2 is approximately 0.99 in the first part of the curve and even closer to one in the second part of the graph.

Coming back to the adjusted parameters described in Table S2, one may observe that four parameters k_1 , k_2 , θ_1 and T_0 have robust values with respect to patients while the parameter θ_2 depends on the patient. Using average values of adjusted parameters on the set of malariatherapy data, we derive the following clinical formula:

$$G(t) = \begin{cases} 3.843 \times 10^7 \cdot P(t-2)^{+1.0304} & \text{if } 2 < t \leq \bar{T}_0 \text{ days,} \\ 2.981 \times 10^9 \cdot P(t)^{-0.0470} & \text{if } \bar{T}_0 \leq t \leq 30 \text{ days,} \end{cases} \quad (10)$$

with $\bar{T}_0 = 14.5636 \pm 0.0064$ days. The relative error for (10) is such that $|\frac{\Delta G}{G}|^2 \leq 2.3884 \times 10^{-4} + 1.0617 |\frac{\Delta P}{P}|^2$, where $|\frac{\Delta P}{P}|$ is the relative error on the measurement of parasitemia. Therefore, if $|\frac{\Delta P}{P}| \leq 5\%$, then $|\frac{\Delta G}{G}| < 5.38\%$. From practical point of view, notice that formula (10) can be really useful to estimate the gametocyte density from the parasitemia measurement without necessarily use the quite ‘complex’ mathematical model described in this note.

4 Discussion

Many models of within-host malaria infection dynamics have been formulated since the pioneer work of Anderson *et al.* [3] in 1989. These models are based on dynamical systems, with standard approaches ranging from ordinary differential equations (ODEs), to delay differential equations (DDEs) or partial differential equations (PDEs). Most ODE model formulations [21, 23–25, 30, 37, 38] assume an exponential process to describe the rate of pRBCs rupture and therefore fail to capture realistic lifetimes of the pRBCs. This issue is somewhat corrected when pRBC sequestration and rupture is modeled either by a set of K -compartments ODEs [21, 26, 41, 48], or DDEs [9, 19, 25, 28]. Other approaches are the use of PDEs to track the infection history of a pRBC [4, 13, 14, 29]. Using gametocyte production as a proxy variable and malariatherapy data, we found that a PDE model outperforms the K -compartments ODEs. Further, the PDE model highlights a strong qualitative connection between gametocyte density and parasitemia which is difficult to capture by the K -compartments ODEs model.

Reducing infections in mosquitoes—vectors of *Plasmodium* parasites—is a crucial component of global efforts to control and eliminate malaria [2]. Because a strong correlation exists between the gametocyte density within a host and infectivity to mosquitoes [7, 11, 12, 22], progress towards this goal would be bolstered by quantifying gametocytes and identifying highly infectious hosts [8, 45, 46]. On the other hand, parasitemia is easily quantified by light microscopy and therefore is more technically accessible, particularly in regions where malaria is endemic. So, quantifying the relationship between the gametocyte density and parasitemia is of great interest to define more simple tools for the prediction of mosquito infection. The results presented in this note provide one such tool.

From a public health or population dynamics point of view, the time course of disease within a host is strongly related to the so-called basic reproduction number, denoted by \mathcal{R}_0 . The \mathcal{R}_0 is defined as the number of secondary infection from a single infected individual introduced in a fully susceptible population. This important metric can be estimated from real data but also using mathematical models. The simplest (deterministic) mathematical model reads as the Ross system of equations from which one can compute this threshold number \mathcal{R}_0 as follows:

$$\mathcal{R}_0 = \mathcal{R}_0^{VH} \times \mathcal{R}_0^{HV} \text{ with } \begin{cases} \mathcal{R}_0^{VH} = abd_M, \\ \mathcal{R}_0^{HV} = macd_H. \end{cases}$$

In the above formula, m represents the number of mosquitoes per person, a denotes the mosquito biting rate, b and c denote the per bite transmission probability respectively from mosquito to human and from human to mosquito, while d_H and d_M correspond respectively to the human recovery and the mosquito death rates. Although more ingredients can be included into the mathematical model, leading to different formulations for \mathcal{R}_0 , the above expression contains the main important parameters [32, 33, 43]. Parameters b and c serve as the link between within- and between-host dynamics, since transmission rates from (to) a host will depend on the dynamics of what is happening within that host (vector). Further, there is a clear relationship between gametocyte density (G) and the transmission probability per bite from human to mosquito (c) [6, 7, 11, 12, 17, 27, 44]. From a practical point of view, the parameter c is difficult to estimate in a relevant way. Indeed, an efficient measurement of c requires a good measure of the gametocyte density which is quite difficult to obtain in practice. So, a simple way to estimate the gametocyte density will help to infer the parameter c . Thanks to formula (9) proposed here, we then have a robust relationships between the parasitemia (easier to measure) and gametocyte density, at least during the first days of infections (approximately the first two weeks).

Overall, the proposed model for the dynamics of gametocytes is certainly valid for the first asexual wave which last approximately 40 days for each patient in this malaria therapy dataset. This relative short term validation is enough for the aim of the current study. However, for the longterm gametocyte dynamics, we need to bring more complexity in the model proposed here. Indeed, the conversion probability of asexual parasites to circulating gametocytes (α_G) should be considered to vary among successive waves of asexual parasitaemia to tackle such issue of the longterm gametocyte dynamics [18], particularly since smear-positive asymptomatic malaria infections detectable by microscopy are an important gametocytes reservoir and often persist for months [31].

The robustness of the model proposed here, especially the formula linking parasitaemia and gametocyte density, is only guaranteed during the first two weeks after infection. Be-

yond this time, this estimate is highly variable from one patient to another. This variability is explained, at least in part, by the variability of the duration of sexual stage ($1/\mu_G$) which governs the decrease in gametocyte density (Table S1). One interpretation of the variation in this parameter is that there exists variation in how well individuals clear gametocytes or kill them through immune responses [16, 31]. Less variability is expected at the beginning of infections, where the whole system is less constrained by immunity. This is likely to be true for the malariatherapy patient data presented here, since hosts were initially naive. However in high transmission settings, acquired immunity—particularly in older hosts—may obscure the relationship between early gametocyte and asexual parasite densities our work has revealed. Further fine scale, longitudinal data could assess the applicability of this relationship across settings and age groups, although such data is understandably difficult to obtain.

Finally, while our work reveals a simple tool for linking aspects of the early dynamics of malaria infections, it also offers specific suggestions for how best to mathematically describe those infection dynamics more broadly. Both PDE and K -compartments ODE models have been adopted to capture some the subtleties of malaria parasite life cycles in blood-stage infections [29]. Our work provides more evidence that, among those choices, PDE models offer clear advantages.

Table 1: Fixed model parameters

Parameters	Description	Values	References
Λ_0	Production rate of RBC	1.73×10^6 RBC/h/ml	[3, 35]
$1/\mu_{r \rightarrow m}$	Duration of the RBC reticulocyte stage	36 h	[34]
$1/\mu_{m \rightarrow s}$	Duration of the RBC mature stage	116.5 days	[34]
$1/\mu_{s \rightarrow d}$	Duration of the RBC senescent stage	48 h	[34]
β	Infection rate of uRBC	6.27×10^{-10} RBC/ml/day	[3]
d_0	Natural death rate of uRBC	0.00833 RBC $\cdot \text{day}^{-1}$	[3]
μ_m	Decay rates of malaria parasites	48 RBC $\cdot \text{day}^{-1}$	[24]
α_G	Proportion of asexual merozoites	0.05	[35]
S_I^*	Innate IR density that gives 50% of parasite killing	$2,755$ cells $\cdot \mu l^{-1}$	[15]
S_A^*	Adaptive IR density that gives 50% of parasite killing	20.4 cells $\cdot \mu l^{-1}$	[15]
Δ_0	Delay required by adaptive IR to be effective	16 days	[15]

Table 2: Initial values for the model

Variables	Description	Initial Values
$R_r(0)$	Population of reticulocytes RBC	62×10^6 RBC $\cdot \text{ml}^{-1}$
$R_m(0)$	Population of mature RBC	4.85×10^9 RBC $\cdot \text{ml}^{-1}$
$R_s(0)$	Population of senescent RBC	83×10^6 RBC $\cdot \text{ml}^{-1}$
$p(0, \cdot)$	Population of pRBC for the PDE model	0 cells $\cdot \text{ml}^{-1}$
p_j	Population of pRBC for the ODE model	0 cells $\cdot \text{ml}^{-1}$
$G(0)$	Population of mature gametocyte	0 cells $\cdot \text{ml}^{-1}$
$m(0)$	Population of malaria parasites	variable

Acknowledgements

Authors thank Samuel Alizon, Laurence Ayong, Carole Eboumbou and Christophe Rogier for comments and suggestions to improve the manuscript.

References

- [1] P. Alano and R. Carter. Sexual differentiation in malaria parasites. *Annual Review of Microbiology*, 44(1):429–449, Oct. 1990.
- [2] P. L. Alonso, G. Brown, M. Arevalo-Herrera, F. Binka, C. Chitnis, F. Collins, O. K. Doumbo, B. Greenwood, B. F. Hall, M. M. Levine, K. Mendis, R. D. Newman, C. V. Plowe, M. H. Rodríguez, R. Sinden, L. Slutsker, and M. Tanner. A Research Agenda to Underpin Malaria Eradication. *PLOS Medicine*, 8(1):e1000406, Jan. 2011.
- [3] R. M. Anderson, R. M. May, and S. Gupta. Non-linear phenomena in host-parasite interactions. *Parasitology*, 99 Suppl:S59–79, 1989.
- [4] R. Antia, A. Yates, and J. C. de Roode. The dynamics of acute malaria infections. I. Effect of the parasite’s red blood cell preference. *Proceedings of the Royal Society B: Biological Sciences*, 275(1641):1449–1458, June 2008.
- [5] L. Bannister and G. Mitchell. The ins, outs and roundabouts of malaria. *Trends in Parasitology*, 19(5):209–213, May 2003.
- [6] T. Bousema, R. R. Dinglasan, I. Morlais, L. C. Gouagna, T. van Warmerdam, P. H. Awono-Ambene, S. Bonnet, M. Diallo, M. Coulibaly, T. Tchuinkam, B. Mulder, G. Targett, C. Drakeley, C. Sutherland, V. Robert, O. Doumbo, Y. Touré, P. M. Graves, W. Roeffen, R. Sauerwein, A. Birkett, E. Locke, M. Morin, Y. Wu, and T. S. Churcher. Mosquito Feeding Assays to Determine the Infectiousness of Naturally Infected *Plasmodium falciparum* Gametocyte Carriers. *PLOS ONE*, 7(8):e42821, Aug. 2012.
- [7] T. Bousema and C. Drakeley. Epidemiology and Infectivity of *Plasmodium falciparum* and *Plasmodium vivax* Gametocytes in Relation to Malaria Control and Elimination. *Clinical Microbiology Reviews*, 24(2):377–410, Apr. 2011.
- [8] T. Bousema and C. Drakeley. Determinants of Malaria Transmission at the Population Level. *Cold Spring Harbor Perspectives in Medicine*, 7(12), Dec. 2017.
- [9] P. Cao, K. A. Collins, S. Zaloumis, T. Wattanakul, J. Tarning, J. A. Simpson, J. McCarthy, and J. M. McCaw. Modeling the dynamics of *Plasmodium falciparum* gametocytes in humans during malaria infection. *eLife*, 8:e49058, Oct. 2019.
- [10] E. Chernin. The Malariatherapy of Neurosyphilis. *The Journal of Parasitology*, 70(5):611–617, 1984.
- [11] T. S. Churcher, T. Bousema, M. Walker, C. Drakeley, P. Schneider, A. L. Ouédraogo, and M.-G. Basáñez. Predicting mosquito infection from *Plasmodium falciparum* gametocyte density and estimating the reservoir of infection. *eLife*, 2:e00626, May 2013.

- [12] W. E. Collins and G. M. Jeffery. A retrospective examination of mosquito infection on humans infected with *Plasmodium falciparum*. *The American Journal of Tropical Medicine and Hygiene*, 68(3):366–371, Mar. 2003.
- [13] D. Cromer, J. Stark, and M. P. Davenport. Low red cell production may protect against severe anemia during a malaria infection—Insights from modeling. *Journal of Theoretical Biology*, 257(4):533–542, Apr. 2009.
- [14] R. D. Demasse and A. Ducrot. An Age-Structured Within-Host Model for Multistrain Malaria Infections. *SIAM Journal on Applied Mathematics*, 73(1):572–593, Jan. 2013.
- [15] K. Dietz, G. Raddatz, and L. Molineaux. Mathematical model of the first wave of plasmodium falciparum asexual parasitemia in non-immune and vaccinated individuals. *The American Journal of Tropical Medicine and Hygiene*, 75(2_suppl):46–55, Aug. 2006.
- [16] D. L. Doolan, C. Dobaño, and J. K. Baird. Acquired Immunity to Malaria. *Clinical Microbiology Reviews*, 22(1):13–36, Jan. 2009.
- [17] C. J. Drakeley, I. Secka, S. Correa, B. M. Greenwood, and G. A. Targett. Host haematological factors influencing the transmission of *Plasmodium falciparum* gametocytes to *Anopheles gambiae* s.s. mosquitoes. *Tropical medicine & international health: TM & IH*, 4(2):131–138, Feb. 1999.
- [18] M. Eichner, H. H. Diebner, L. Molineaux, W. E. Collins, G. M. Jeffery, and K. Dietz. Genesis, sequestration and survival of *Plasmodium falciparum* gametocytes: Parameter estimates from fitting a model to malariatherapy data. *Transactions of The Royal Society of Tropical Medicine and Hygiene*, 95(5):497–501, Sept. 2001.
- [19] L. L. Fonseca and E. O. Voit. Comparison of Mathematical Frameworks for Modeling Erythropoiesis in the Context of Malaria Infection. *Mathematical biosciences*, 270(00):224–236, Dec. 2015.
- [20] U. Frevert. Sneaking in through the back entrance: The biology of malaria liver stages. *Trends in Parasitology*, 20(9):417–424, Sept. 2004.
- [21] M. B. Gravenor and A. L. Lloyd. Reply to: Models for the in-host dynamics of malaria revisited: Errors in some basic models lead to large over-estimates of growth rates. *Parasitology*, 117(5):409–410, Nov. 1998.
- [22] P. M. Graves, T. R. Burkot, R. Carter, J. A. Cattani, M. Lagog, J. Parker, B. J. Brabin, F. D. Gibson, D. J. Bradley, and M. P. Alpers. Measurement of malarial infectivity of human populations to mosquitoes in the Madang area, Papua New Guinea. *Parasitology*, 96(2):251–263, Apr. 1988.
- [23] B. Hellriegel. Modelling the immune response to malaria with ecological concepts: Short-term behaviour against long-term equilibrium. *Proceedings of the Royal Society of London. Series B: Biological Sciences*, 250(1329):249–256, Dec. 1992.
- [24] C. Hetzel and R. M. Anderson. The within-host cellular dynamics of bloodstage malaria: Theoretical and experimental studies. *Parasitology*, 113 (Pt 1):25–38, July 1996.

- [25] M. B. Hoshen, R. Heinrich, W. D. Stein, and H. Ginsburg. Mathematical modelling of the within-host dynamics of *Plasmodium falciparum*. *Parasitology*, 121 (Pt 3):227–235, Sept. 2000.
- [26] A. Iggidr, J.-C. Kamgang, G. Sallet, and J.-J. Tewa. Global Analysis of New Malaria Intrahost Models with a Competitive Exclusion Principle. *SIAM Journal on Applied Mathematics*, 67(1):260–278, Jan. 2006.
- [27] G. L. Johnston, D. L. Smith, and D. A. Fidock. Malaria’s Missing Number: Calculating the Human Component of R_0 by a Within-Host Mechanistic Model of *Plasmodium falciparum* Infection and Transmission. *PLOS Computational Biology*, 9(4):e1003025, Apr. 2013.
- [28] D. H. Kerlin and M. L. Gatton. Preferential Invasion by *Plasmodium* Merozoites and the Self-Regulation of Parasite Burden. *PLOS ONE*, 8(2):e57434, Feb. 2013.
- [29] D. S. Khoury, R. Aogo, G. Randriafanomezantsoa-Radohery, J. M. McCaw, J. A. Simpson, J. S. McCarthy, A. Haque, D. Cromer, and M. P. Davenport. Within-host modeling of blood-stage malaria. *Immunological Reviews*, 285(1):168–193, 2018.
- [30] Y. Li, S. Ruan, and D. Xiao. The within-host dynamics of malaria infection with immune response. *Mathematical biosciences and engineering: MBE*, 8(4):999–1018, Oct. 2011.
- [31] J. T. Lin, D. L. Saunders, and S. R. Meshnick. The role of submicroscopic parasitemia in malaria transmission: What is the evidence? *Trends in Parasitology*, 30(4):183–190, Apr. 2014.
- [32] G. Macdonald. The Measurement of Malaria Transmission. *Proceedings of the Royal Society of Medicine*, 48(4):295–302, Apr. 1955.
- [33] S. Mandal, R. R. Sarkar, and S. Sinha. Mathematical models of malaria - a review. *Malaria Journal*, 10(1):202, July 2011.
- [34] P. G. McQueen and F. E. McKenzie. Host Control of Malaria Infections: Constraints on Immune and Erythropoietic Response Kinetics. *PLOS Computational Biology*, 4(8):e1000149, Aug. 2008.
- [35] P. G. McQueen, K. C. Williamson, and F. E. McKenzie. Host immune constraints on malaria transmission: Insights from population biology of within-host parasites. *Malaria Journal*, 12(1):206, June 2013.
- [36] L. H. Miller, H. C. Ackerman, X.-z. Su, and T. E. Wellems. Malaria biology and disease pathogenesis: Insights for new treatments. *Nature medicine*, 19(2):156–167, Feb. 2013.
- [37] J. L. Mitchell and T. W. Carr. Oscillations in an Intra-host Model of *Plasmodium Falciparum* Malaria Due to Cross-reactive Immune Response. *Bulletin of Mathematical Biology*, 72(3):590–610, Apr. 2010.
- [38] L. Molineaux and K. Dietz. Review of intra-host models of malaria. *Parassitologia*, 41(1-3):221–231, Sept. 1999.

- [39] R. E. L. Paul, F. Ariey, and V. Robert. The evolutionary ecology of *Plasmodium*. *Ecology Letters*, 6(9):866–880, 2003.
- [40] R. C. Russell, D. Otranto, and R. L. Wall. *The Encyclopedia of Medical and Veterinary Entomology*. CABI, 2013.
- [41] S. Saralamba, W. Pan-Ngum, R. J. Maude, S. J. Lee, J. Tarning, N. Lindegårdh, K. Chotivanich, F. Nosten, N. P. J. Day, D. Socheat, N. J. White, A. M. Dondorp, and L. J. White. Intra-host modeling of artemisinin resistance in *Plasmodium falciparum*. *Proceedings of the National Academy of Sciences*, 108(1):397–402, Jan. 2011.
- [42] A. Saul. Models for the in-host dynamics of malaria revisited: Errors in some basic models lead to large over-estimates of growth rates. *Parasitology*, 117(5):405–407, Nov. 1998.
- [43] D. L. Smith, K. E. Battle, S. I. Hay, C. M. Barker, T. W. Scott, and F. E. McKenzie. Ross, macdonald, and a theory for the dynamics and control of mosquito-transmitted pathogens. *PLoS pathogens*, 8(4):e1002588, 2012.
- [44] K. Stepniewska, R. N. Price, C. J. Sutherland, C. J. Drakeley, L. von Seidlein, F. Nosten, and N. J. White. *Plasmodium falciparum* gametocyte dynamics in areas of different malaria endemicity. *Malaria Journal*, 7(1):249, Dec. 2008.
- [45] W. Stone, B. P. Gonçalves, T. Bousema, and C. Drakeley. Assessing the infectious reservoir of *falciparum* malaria: Past and future. *Trends in Parasitology*, 31(7):287–296, July 2015.
- [46] T. m. R. C. P. o. C. t. R. a. M. Transmission. malERA: An updated research agenda for characterising the reservoir and measuring transmission in malaria elimination and eradication. *PLOS Medicine*, 14(11):e1002452, Nov. 2017.
- [47] World Health Organization. *World Malaria Report 2019*. World Health Organization, S.I., 2019.
- [48] S. Zaloumis, A. Humberstone, S. A. Charman, R. N. Price, J. Moehrle, J. Gamobenito, J. McCaw, K. M. Jansen, K. Smith, and J. A. Simpson. Assessing the utility of an anti-malarial pharmacokinetic-pharmacodynamic model for aiding drug clinical development. *Malaria Journal*, 11(1):303, Aug. 2012.

A Supplementary figures

Figure S1: Comparison with data and mathematical model output for gametocyte density for other patients.

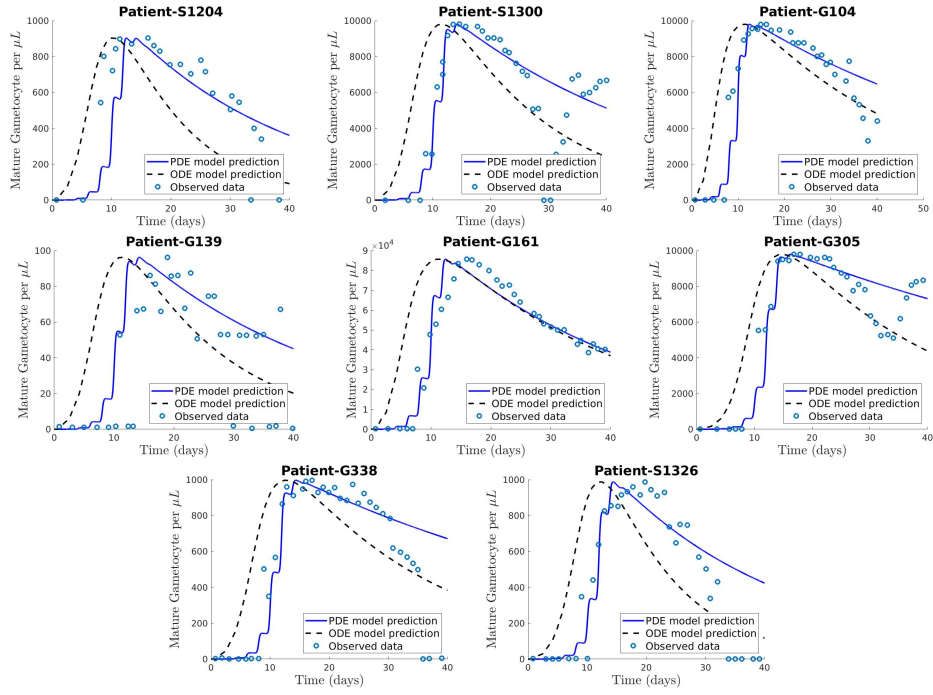


Figure S2: The time evolution parasitemia and gametocyte density curves computed from the PDE model for other patients.

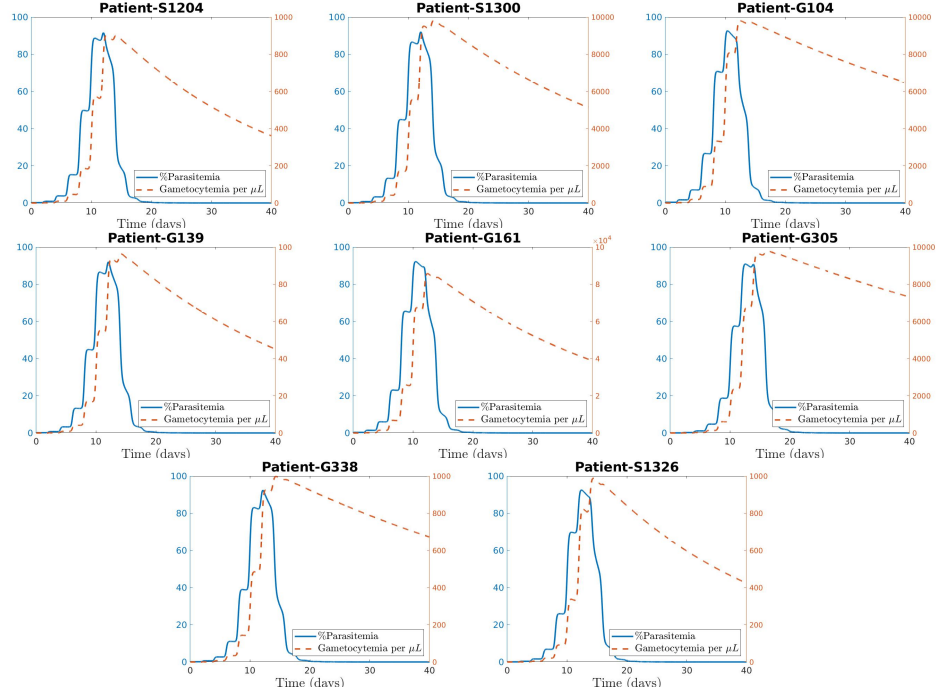
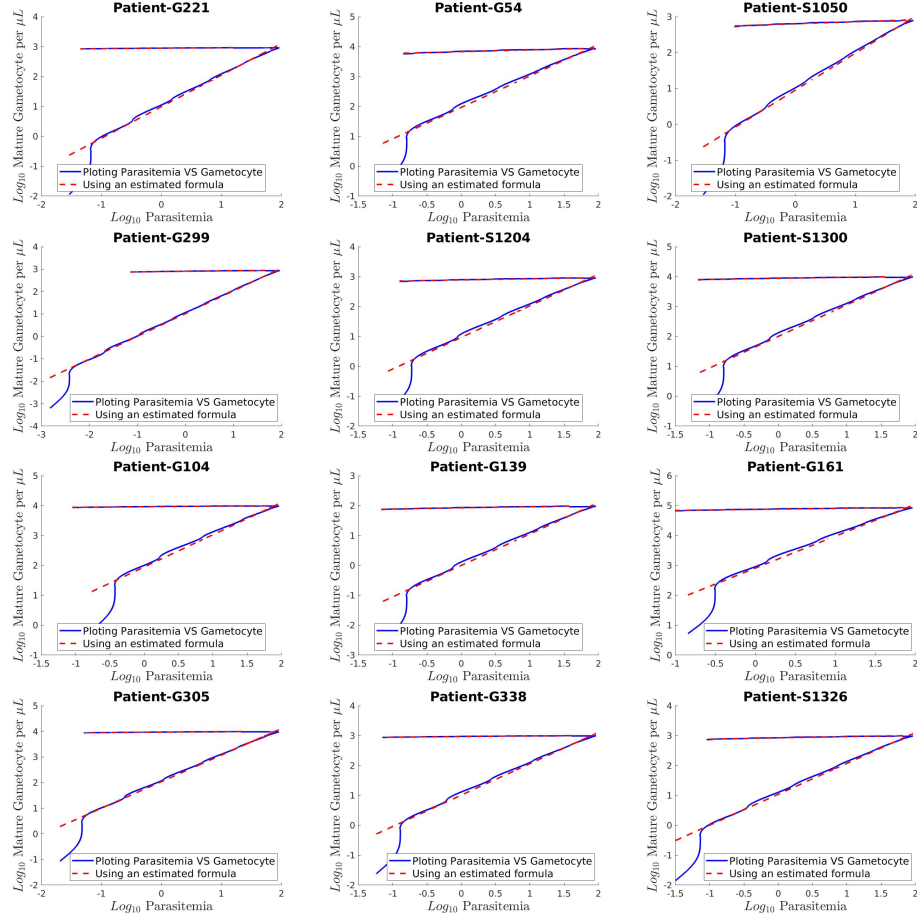


Figure S3: Comparison between model prediction and the linear regression based on formula (9)



B Supplementary tables

Table S1: Patient-specific parameters estimated from the data

	G54	G221	S1050	S1204	S1300	G104
$\mu_G(\times 10^{-3})$	2.27	0.4632	1.99	1.5	1.07	0.667
$\alpha_G(\times 10^{-8})$	13.02	1.206	1.161	1.289	13.47	13.02
$m_0(\times 10^7)$	2.5	1	1	2.97	2.5	6
	G139	G161	G305	G338	G299	S1326
$\mu_G(\times 10^{-3})$	1.25	1.25	0.526	0.667	0.80	1.43
$\alpha_G(\times 10^{-8})$	0.134	118.57	12.84	1.321	1.1682	1.382
$m_0(\times 10^7)$	2.5	5	0.7	2	0.05	1.1

Table S2: Estimated parameters for the shape (9)

	G221	G54	S1050	S1204
$\log_{10}(k_1)$	2.9586 ± 0.0037	2.9326 ± 0.0039	2.9520 ± 0.0037	2.9502 ± 0.0037
θ_1	1.0321 ± 0.0028	1.0312 ± 0.0030	1.0315 ± 0.0029	1.0315 ± 0.0028
$\log_{10}(k_2)$	2.9437 ± 0.0002	3.8802 ± 0.0005	2.9101 ± 0.0004	2.9148 ± 0.0003
θ_2	-0.0141 ± 0.0004	-0.0477 ± 0.0005	-0.0336 ± 0.0005	-0.0280 ± 0.0003
$T_0(\text{days})$	14.7125 ± 0.0075	13.2917 ± 0.0083	14.4958 ± 0.0083	13.4666 ± 0.0025
	S1300	G104	G139	G161
$\log_{10}(k_1)$	2.9861 ± 0.0037	2.9821 ± 0.0041	2.8024 ± 0.0037	2.9272 ± 0.0039
θ_1	1.0315 ± 0.0028	1.0304 ± 0.0031	1.0315 ± 0.0028	1.0312 ± 0.0029
$\log_{10}(k_2)$	3.9442 ± 0.0003	3.9663 ± 0.0002	1.9360 ± 0.0003	4.8774 ± 0.0002
θ_2	-0.0336 ± 0.0003	-0.0170 ± 0.0002	-0.0336 ± 0.0003	-0.0214 ± 0.0003
$T_0(\text{days})$	14.5375 ± 0.0075	13.2625 ± 0.0083	14.5625 ± 0.0083	13.3875 ± 0.0025
	G299	G305	G338	S1326
$\log_{10}(k_1)$	2.9712 ± 0.0034	2.9854 ± 0.0037	2.9897 ± 0.0041	2.9893 ± 0.0037
θ_1	1.0301 ± 0.0027	1.0315 ± 0.0028	1.0304 ± 0.0031	1.0315 ± 0.0028
$\log_{10}(k_2)$	2.9063 ± 0.0003	3.9607 ± 0.0001	2.9739 ± 0.0002	2.9474 ± 0.0003
θ_2	-0.0203 ± 0.0003	-0.0188 ± 0.0002	-0.0170 ± 0.0002	-0.0336 ± 0.0003
$T_0(\text{days})$	20.0083 ± 0.0075	14.6917 ± 0.0083	14.2625 ± 0.0083	14.5458 ± 0.0025